Received 22 February 2024; revised 8 May 2024 and 19 June 2024; accepted 20 June 2024. Date of publication 28 June 2024; date of current version 15 November 2024. The review of this article was arranged by Editor Paolo Bonato.

Digital Object Identifier 10.1109/OJEMB.2024.3420247

Scalable Neuroanatomical and Behavioral Phenotyping of Radio Frequency Radiation on Young Zebrafish

XIAOLI WU [1], YU SUEN CHAN [2], BINGJIE XIANG [1] (Member, IEEE), WENHUI ZHANG [1], KWAI-MAN LUK [1] (Life Fellow, IEEE), SHUK HAN CHENG [2], YUK FAI LEUNG [3], AND ROSA H. M. CHAN [1] (Senior Member, IEEE)

[1]State Key Laboratory of Terahertz and Millimeter Waves, Department of Electrical Engineering, City University of Hong Kong, Hong Kong, SAR, China
[2]Department of Biomedical Sciences, City University of Hong Kong, Hong Kong, SAR, China
[3]Department of Biological Sciences, Purdue University, West Lafayette, IN 47907 USA

CORRESPONDING AUTHOR: ROSA H. M. CHAN (e-mail: rosachan@cityu.edu.hk).

This work was supported by the Research Grants Council of the Hong Kong Special Administrative Region, and China under Project CityU 11217019.
This article has supplementary downloadable material available at https://doi.org/10.1109/OJEMB.2024.3420247, provided by the authors.

ABSTRACT *Objective:* In our wireless-centric world, evaluating the health effects of radio frequency electromagnetic radiation (RF-EMR) is crucial. An existing research gap pertains to the replication of real-world specific absorption rates (SAR) for RF-EMR, especially within aquatic environments. We aimed to bridge this gap using an innovative TEM cell platform to replicate realistic SAR conditions in water and assess RF-EMR's impact on neuroanatomical and behavioral changes. *Results:* We examined RF-EMR effects on zebrafish embryos exposed to RF-EMR during the 4-58 hours post-fertilization phase. Temporary neuroanatomical enlargements and minor behavioral shifts were observed, diminishing by day 8 post-fertilization. *Conclusion:* Short-term RF-EMR exposure at tested levels did not yield significant long-term effects. Nevertheless, investigating prolonged exposure remains imperative. Our study serves as a pioneering model for future investigations into the biological consequences of RF-EMR exposure, highlighting the importance of assessing its health implications in our wireless-centric world

INDEX TERMS Behavioral effects, electromagnetic exposure, high-throughput analysis, zebrafish.

IMPACT STATEMENT This study established a novel and scalable platform for evaluating RF-EMR effects on aquatic life, providing valuable insights into short-term exposure outcomes, advancing scientific understanding in this critical field.

I. INTRODUCTION

Radio frequency (RF) radiation is a form of non-ionizing electromagnetic radiation emitted by various devices, such as mobile phones, Wi-Fi routers, and radio and television broadcasts. With the growing ubiquity of wireless technologies, concerns about potential health risks have spurred interest in understanding the effects of RF radiation on human physiology and behavior [1], [2], [3].

RF fields have thermal effects, such as tissue heating and potential burns with high, prolonged exposures [4], and non-thermal effects that influence cellular processes even at low, chronic exposure levels. Although RF fields do not directly damage DNA [5], they can affect ion fluxes, generate reactive oxygen species, disrupt calcium metabolism, and alter gene expression [6], [7]. Studies on brain metabolism show minor regional changes due to mobile phone use [8], and research on fertility reveals reduced fertility in both sexes, with varied effects on sperm and female reproductive health [9], [10], [11], [12].

The widespread adoption of modern wireless technology has significantly heightened our exposure to RF electromagnetic fields [13]. As devices such as smartphones, Wi-Fi

routers, and IoT gadgets are used more frequently and are kept closer to our bodies, our personal RF exposure increases. Moreover, the long-term health effects of this chronic, low-level exposure remain poorly understood.

Zebrafish serve as a valuable model organism for studying RF radiation effects due to their rapid development, transparency, high fecundity, and wide applicability in diverse research areas. Previous research on the effects of RF radiation on zebrafish has provided valuable insights, but has also faced limitations.

Piccinetti et al. demonstrated that 100 MHz RF-EMR led to developmental disruptions in zebrafish embryos, including growth reduction and an increase in oxidative stress gene transcription, with some recovery by 72 hpf [14]. However, the study focused exclusively on the 100 MHz frequency, which may not be representative of the frequencies used in modern smartphones and IoT devices, limiting the scope of the research. Another study by [15] observed minimal impact of 3.5 GHz RF-EMR on zebrafish embryos, with a slight reduction in startle response. However, the SAR was estimated by the power density at the water surface of the zebrafish embryo medium, while the actual exposure submerged the water could be considerably lower than reported due to attenuation. Research conducted by [16] reported a developmental delay at ultra-high-frequency (UHF, 900 MHz) electromagnetic radiation exposure, but the study focused narrowly on the response of melanophores, not fully addressing potential health risks. Furthermore, the actual SAR experienced by the zebrafish embryos submerged in water was not calculated. Guo et al. found that low-frequency (50 Hz) exposure altered larval movement and brain structure [17]. However, as the detrimental effects of RF-EMR depend on its frequency and intensity, any extrapolation of findings from low-frequency electromagnetic radiation to radio frequency radiation must be approached with caution.

The importance of understanding the impacts of RF-EMR, especially under real-world conditions, cannot be overstated. To achieve a comprehensive understanding, it is crucial to study frequencies that are commonly encountered in everyday life. These studies should adhere to the upper limits for SAR and electric field intensities while encompassing both behavioral and morphological changes. By adopting such an approach, we can gain deeper insights into the effects of RF-EMR and obtain valuable information regarding its potential implications for human health.

In our current study, we aimed to address these critical considerations. We developed a platform that consists of two major components: the RF-EMR radiation system and the zebrafish monitoring system. The radiation system was carefully designed to account for the attenuation of power from air to water. This setup allowed us to closely replicate the desired exposure levels beneath the water. In this way, the radiation exposure could closely mimic our targeted exposure level. The zebrafish monitoring system, on the other hand, was designed to detect subtle changes in behavior and morphology related to neural development. It demonstrated high sensitivity and robustness, particularly in assessing morphological and behavioral alterations.

To streamline our study, we primarily focused on the 900 MHz frequency, commonly utilized in various wireless technologies, such as the Global System for Mobile Communications (GSM). While we specifically examined one frequency, our platform is scalable and adaptable to different frequency ranges and power inputs as needed. We can adjust the frequency and power inputs to meet the required SAR levels. In designing our exposure levels beneath the water, we adhered to the upper safety limits for public exposure from cellular telephones set by both the Federal Communications Commission (FCC) in the USA [18] and the International Commission on Non-Ionizing Radiation Protection (ICNIRP) [19], which are 1.6 W/kg and 2 W/kg, respectively. When an individual maintains a greater distance between their body and the mobile phone, their exposure to radiofrequency radiation decreases significantly [20]. Employing the highest RF band and exposure power levels in day-to-day real-world scenarios allows the experiments capture the most severe exposure scenario in direct contact with the source.

During our investigation, we focused on both behavioral and morphological changes, with a primary emphasis on neuroanatomical and behavioral alterations due to the brain's sensitivity and vulnerability to external influences during development. By studying the effects of RF-EMR on zebrafish brain morphology, we can gain valuable insights into potential impacts on human nervous system. To explore potential modifications in the nervous system and behavior resulting from electromagnetic radiation exposure, we employed a robust behavioral paradigm, specifically the light-induced locomotor response, as previously employed by Gao et al. [21]. This approach facilitated the investigation of potential alterations in the nervous system and behavior, offering a reliable and efficient means of detecting behavioral changes in a high-throughput manner. By structuring our study this way, we provide a more representative understanding of the effects of RF-EMR. For a comprehensive comparison between our study and previous investigations of RF-EMR exposure in zebrafish, please refer to Table 1.

II. RESULTS

A. EXPOSURE SETUP AND CONDITIONS

A TEM cell was employed to generate the required electrical field for our experiments, with detailed information provided in Section V. This arrangement facilitated controlled exposure at two SAR levels: 1.6 W/kg and 2 W/kg. The simulation results of the electric field (Fig. 1B) illustrate its distribution beneath the water surface. In the enlarged view of Fig. 1B, the uniform electric field inside the embryo container is clearly evident. The coefficient of variation of the SAR is 28.4%, indicating a uniform SAR distribution. Thermal simulations (Fig. 1C) verified that temperatures within the exposure setup

TABLE 1. Summary of Zebrafish Studies Involving RF-EMR Exposure

Study	Start (hpf)	Frequency	Duration (h)	Exposure Level
[14]	0	100 MHz	72	EF: 6 V/m; SAR $< 1 \times 10^{-6}$W/kg
[15]	6	3.5 GHz	42	SAR: 8.27W/kg (water surface)
[16]	1–2	900 MHz	∼120	EF: 71 V/m (input signal)
[17]	3	50Hz	120	MF: 100, 200, 400, and 800 μ T
Ours	4	900 MHz	54	SAR: 1.6W/kg, 2W/kg

Note: All zebrafish used in the previous studies were of the AB line; Our study used Tg(*elavl3:EGFP*)^{knu3} line; EF, electrical field strength; MF, magnetic field; SAR, specific absorption rate

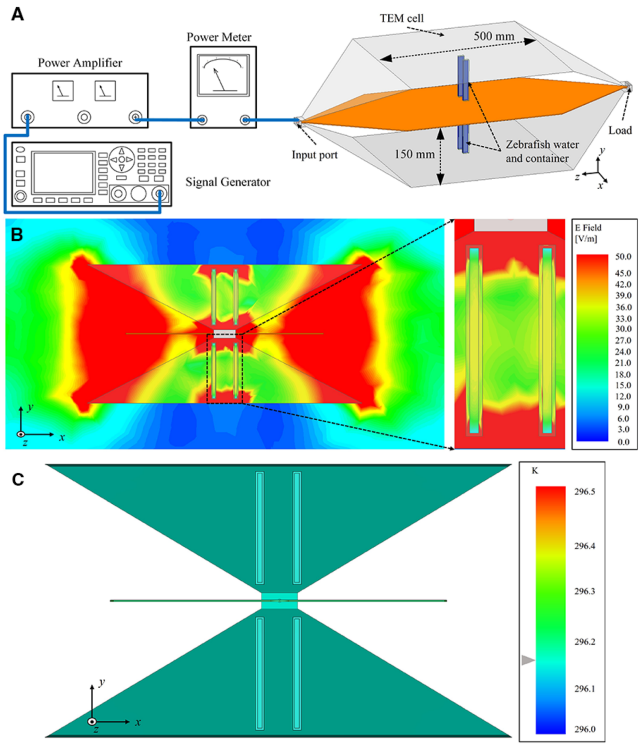

FIGURE 1. An overview of the simulation setup. A: The involved equipment and setup; B: The simulated electrical field distribution within the TEM cell; C: The thermal simulation within the same TEM cell.

remained consistent with environmental conditions. Under these circumstances, embryos from the Tg(*elavl3: EGFP*)^{knu3} zebrafish line were exposed from 4 to 58 hpf.

B. MORPHOLOGY CHANGES

To investigate the effects of RF-EMR exposure on morphology, we evaluated the dimensions of different brain regions (including the entire brain, forebrain, midbrain, and hindbrain) by quantifying fluorescent signal areas from the zebrafish larvae after exposure, during the period from 5 to 8 dpf. This method enables the identification of potential regional vulnerabilities to RF-EMR exposure. Additionally, we measured body size, eye area, and body length to assess overall physical characteristics.

The findings from our study revealed that exposure to an SAR of 2 W/kg resulted in a marginally increased eye size at 5 dpf (Fig. 2E), coupled with an expansion in the whole brain and midbrain size at the same developmental stage (Fig. 3, G and I). Similarly, when exposed to an SAR of 1.6 W/kg, there was an increase in eye size at 5 dpf (Fig. 2B).

However, the aforementioned enlargement in the overall brain and midbrain dimensions, along with the eye area, were transient and did not persist beyond the 5 dpf stage. By the period spanning 6 to 8 dpf, these disparities had vanished. The morphological attributes of the control and radiation groups were indistinguishable during this later developmental phase (Fig. 2 and Fig. 3, 6-8dpf).

C. BEHAVIORAL ANALYSIS

In our experimental setup, we employed a modified LLR protocol based on the one outlined by [21]. This protocol involves alternating light and dark phases (ON-OFF-ON-OFF blocks) and was implemented on zebrafish larvae between 5 to 8 dpf following RF-EMR exposure. By manipulating light conditions sequentially, we elicited a variety of locomotor responses that indicate the behavioral state.

The behavioural anlalysis consits of two main parts: first, we compared the overall locomotor activity by analyzing the bursting activity data between the control and exposed groups. Second, we extracted and compared specific behavioral features from these activities, detailed in Table S1. For additional details on the LLR protocol, behavioral feature extraction, and normalization methods, please refer to Section V.

1) COMPARATIVE ANALYSIS OF PRE-STIMULUS AND POST-STIMULUS ACTIVITIES

In comparing the raw activity data between the control and RF-EMR exposure groups, we conducted statistical analyses separately for pre-stimulus and post-stimulus activities. For the pre-stimulus bursting activity comparisons, no significant differences were found (Table 2). This result is expected, as we performed normalization by subtracting the baseline of batch and well-dependent activities, as well as individual larvae pre-stimulus activities. This normalization procedure ensures that any observed differences post-stimulation are more likely due to the effects of RF-EMR exposure rather than baseline differences in activity.

For the 30-second post-stimulus activities, significant differences were observed on 6 dpf for the first post-light OFF period (p=0.031) in the SAR=1.6 W/kg group and on 5 dpf for the first post-light OFF period (p=0.003) and 6 dpf for the second post-light ON period (p=0.009) in the SAR=2 W/kg

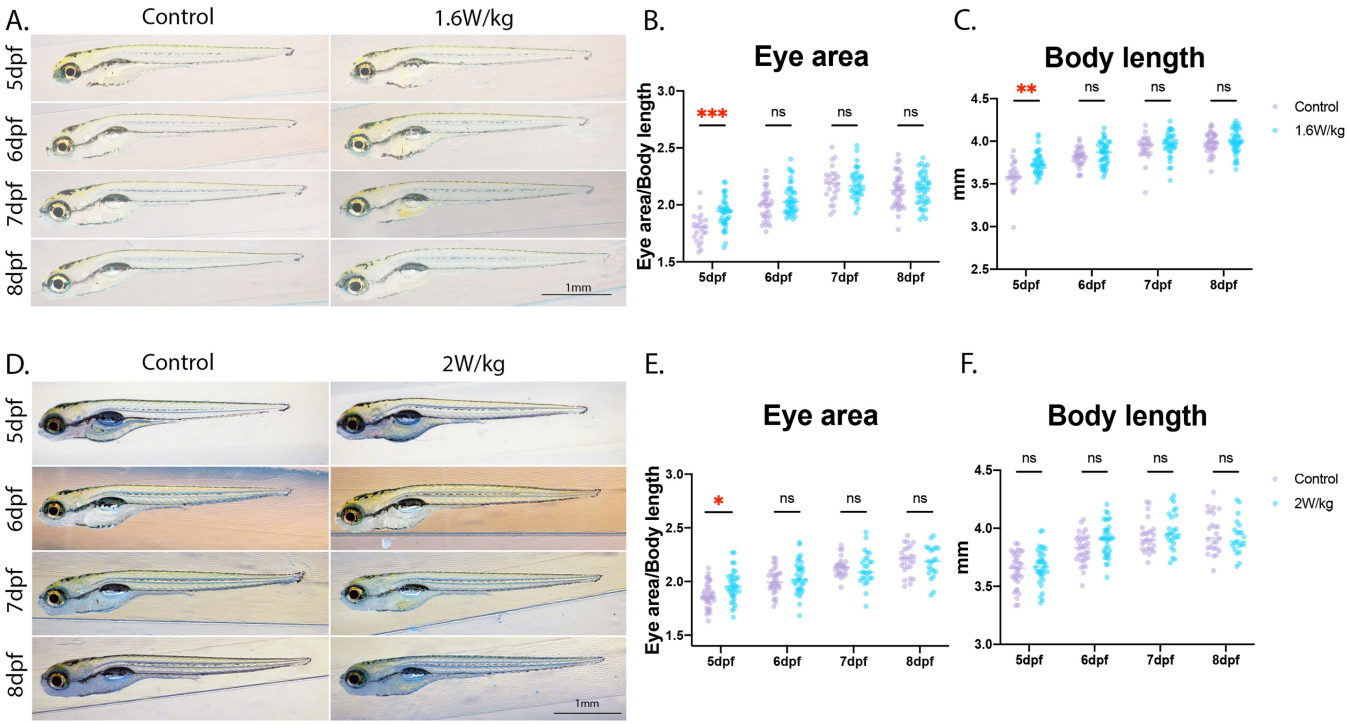

FIGURE 2. The impact of RF-EMR on the development of zebrafish larvae after 54 hours of exposure from 4 hpf to 58 hpf. A: Representative images of zebrafish larvae after exposure to 1.6 W/kg RF-EMR. B: The eye area in zebrafish is measured from 5 dpf to 8 dpf after 1.6 W/kg RF-EMR exposure. Data were adjusted based on body length. C: Measurement of the body length of zebrafish following 1.6 W/kg RF-EMR exposure from 5 dpf to 8 dpf. D: Representative images of zebrafish larvae after exposure to 2 W/kg RF-EMR. E: Measurement of the eye area in zebrafish following 2 W/kg RF-EMR exposure from 5 dpf to 8 dpf. Data were adjusted based on body length. F: Measurement of the body length of zebrafish following 2 W/kg RF-EMR exposure from 5 dpf to 8 dpf. A two-way ANOVA was used for data analysis. Asterisks indicate significant differences between the treatment groups and the control group (*** for $p < 0.001$, ** for $p < 0.01$, and * for $p < 0.05$.).

TABLE 2. Statistical Comparison of Radiation and Control Groups: Power Levels & Days (Pre-Stimulus P-Value / Post-Stimulus P-Value)

Comparison	5dpf	6dpf	7dpf	8dpf
SAR = 1.6W/kg				
1st OFF → ON	0.993/0.410	0.237/0.138	0.527/0.656	0.903/0.855
1st ON → OFF	1.000/0.635	0.349/0.031(*)	0.981/0.295	0.629/0.062
2nd OFF → ON	0.896/0.964	0.258/0.105	0.148/0.301	0.364/0.635
2nd ON → OFF	1.000/0.556	0.664/0.678	0.853/0.178	0.797/0.151
SAR = 2W/kg				
1st OFF → ON	0.575/0.624	0.243/0.365	0.693/0.126	0.755/0.533
1st ON → OFF	0.953/0.003 (**)	0.289/0.449	0.208/0.715	0.740/0.350
2nd OFF → ON	0.653/0.857	0.419/0.009(**)	0.244/0.611	0.907/0.290
2nd ON → OFF	0.998/0.287	0.313/0.847	0.981/0.271	0.963/0.713

group. No significant differences were found between the exposure and control groups on 7 and 8 dpf, regardless of the radiation exposure power level (see table 2).

2) COMPARATIVE ANALYSIS OF BURSTING FEATURES

Since pre- and post-stimulus bursting activity comparisons only evaluate the overall 30-second bursting activities, we further examined bursting activity features such as startle response, active and rest bouts for a more comprehensive comparison. We focused on features extracted from the burst activity data, specifically the initial transition from OFF to ON and vice versa. This was used to minimize potential influences from larvae adapting to the changing light conditions, as we observed differences between the first and second transitions. The specific features extracted for our analysis are detailed in Table S1.

a) Startle Response: Zebrafish larvae did not exhibit obvious vision impairment following exposure to RF-EMR, as evidenced by similar startle responses after light ON in both 1.6 W/kg and 2 W/kg SAR radiation groups. Fig. 4A and 4 B demonstrate that the proportion of zebrafish exhibiting startle responses after light activation is comparable between control and radiation groups from 5 dpf to 8 dpf, in both radiation groups. Additionally, the latency of startle responses among

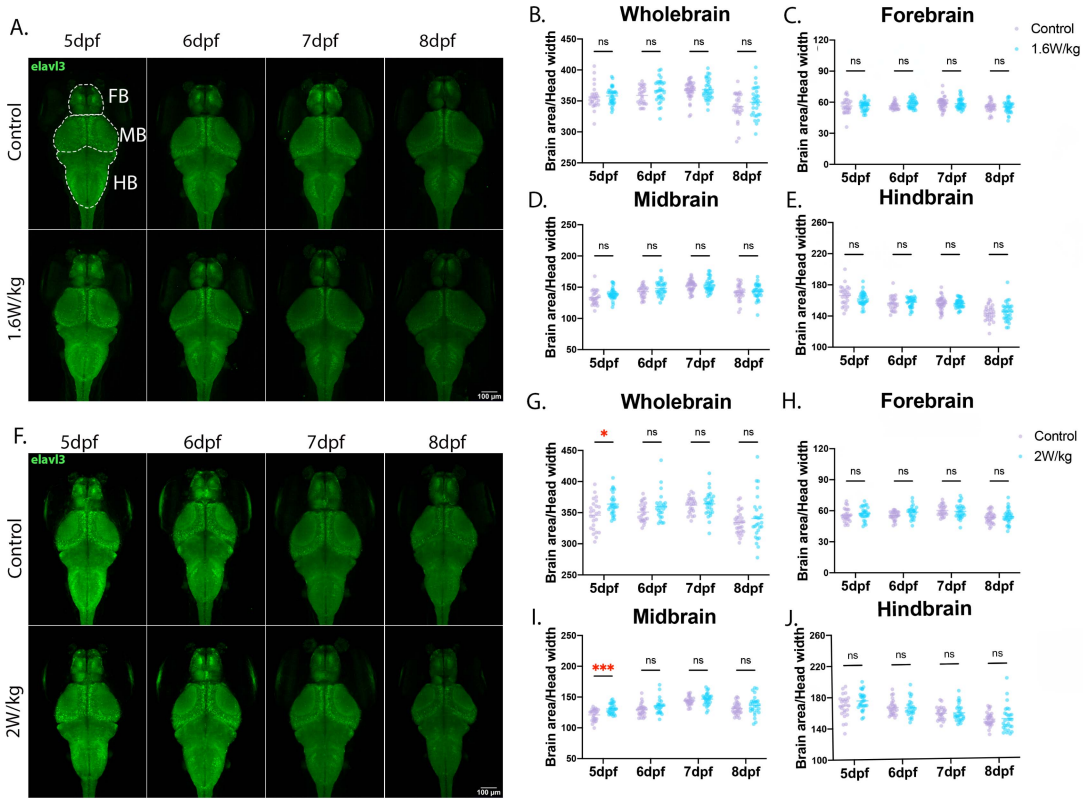

FIGURE 3. **The effects of RF-EMR on the development of zebrafish larvae brain were investigated after 54 hours of exposure, from 4 hpf to 58 hpf. To examine the specific impact of RF-EMR on various regions of the zebrafish brain, we quantified size in the whole brain, forebrain (FB), midbrain (MB), and hindbrain (HB) areas. A: Representative fluorescence images of Tg(*elavl3: EGFP*)^{knu3} zebrafish larvae subsequent to a 1.6 W/kg RF-EMR exposure. B-E: Quantitative analyses of the whole brain, forebrain, midbrain, and hindbrain areas respectively, in zebrafish larvae post 1.6 W/kg RF-EMR exposure, from 5 dpf to 8 dpf. The measurements are normalized to the head width. F: Representative fluorescence images of Tg(*elavl3: EGFP*)^{knu3} zebrafish larvae subsequent to a 2 W/kg RF-EMR exposure. G-J: Quantitative analyses of the whole brain, forebrain, midbrain, and hindbrain areas respectively, in zebrafish larvae post 2.0 W/kg RF-EMR exposure, from 5 dpf to 8 dpf. These measurements are also normalized to the head width. A two-way ANOVA was used for data analysis. Asterisks indicate significant differences between the treatment groups and the control group (*** for $p < 0.001$, and * for $p < 0.05$.).**

zebrafish that exhibited these responses is consistent between radiation and control groups from 5 dpf to 8 dpf, as shown in Fig. 4C and 4 D. The similarity in startle responses suggests that the vision capability of zebrafish larvae is not adversely affected by RF-EMR exposure.

b) Adaptation Time: Following the startle response, zebrafish larvae generally experience a short period of decreased activity before returning to their active state. We assessed the adaptation time from the moment of light activation to when the larvae resumed their active stage. The findings show differences in adaptation times between radiation and control groups, primarily at 5 and 6 dpf across both RF-EMR levels. However, these differences diminished at 7 and 8 dpf, as illustrated in Fig. 4E and 4F. Additionally, we measured the adaptation time from light OFF to when the larvae resumed their rest stage in a dark environment. The adaptation time after light off remained unaffected by both levels of RF-EMR, as displayed in Fig. 4G and 4H.

c) Active and Rest Bouts: The bout count and mean duration are significant indicators of zebrafish larvae's behavioral changes. These two measures show us how often (the frequency) and for how long (the duration) the larvae are active or at rest. Any alterations in these patterns may be a sign of neurological changes in the larvae after being exposed to RF-EMR.

We collected data on these measures during periods of both light and darkness. During the light-on period, we observed that zebrafish in both the low and high RF-EMR groups exhibited increased activity but for shorter durations compared to the control group on 6 and 7dpf, as shown in Fig. 5A-D. This increased activity could suggest higher alertness or even stress levels in these larvae.

Also during the light-on period, these larvae rested less often and for shorter times on the 6 dpf (Fig. 5E-H). This reduced rest might also imply heightened alertness or stress. However, by the 8dpf, these differences in active and rest periods compared to the control group had mostly disappeared.

There was one exception during the light-on period, where we saw the high RF-EMR group taking more frequent but shorter rests on 5dpf (Fig. 5F and 5H). This may again suggest higher alertness levels, but this pattern was not observed in the low radiation group.

During the light-off period, the high radiation group exhibited similar activity and resting behavior to the control group

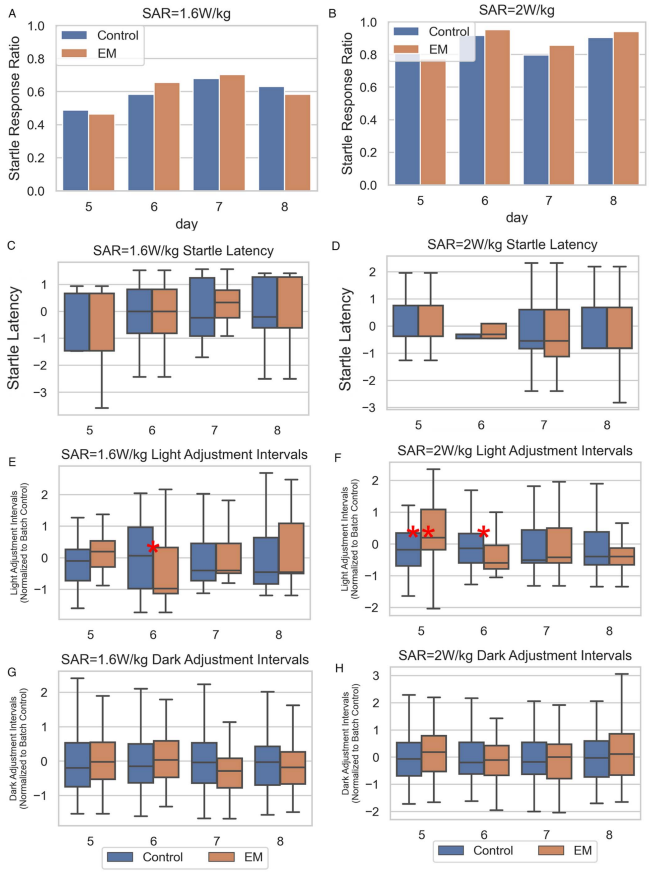

FIGURE 4. **Startle responses and adaptation times of zebrafish larvae subjected to two SAR radiation groups: SAR=1.6 W/kg and SAR=2 W/kg. A-D focus on the startle responses triggered by sudden illumination (light ON). A-B: bar charts displaying the proportion of zebrafish larvae exhibiting startle responses. C-D: boxplots representing the latency of startle responses for zebrafish larvae that exhibit startle reactions. E-H show the larvae's adaptation times, defined as the interval from a change in lighting (either light ON or OFF) to when the larvae resume their normal active or resting behaviors. E-F: adaptation time after light is ON; G-H: adaptation time after light is OFF; Left: SAR=1.6 W/kg; Right: SAR=2 W/kg; Blue: control group; Orange: radiation group. Significance levels are denoted as follows: *** for $p < 0.001$, ** for $p < 0.01$, and * for $p < 0.05$.**

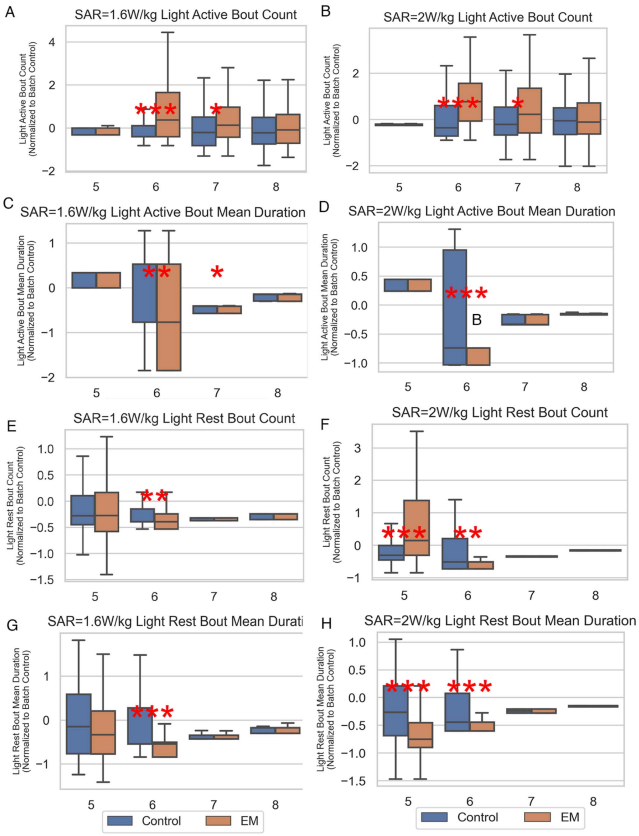

FIGURE 5. **Boxplots illustrating the active and rest bout counts and the mean durations for zebrafish larvae after light ON, at 5, 6, 7, and 8 dpf. Left: SAR=1.6 W/kg; Right: SAR=2 W/kg; Blue: control group; Orange: radiation group. Significance levels are denoted as follows: *** for $p < 0.001$, ** for $p < 0.01$, and * for $p < 0.05$.**

(Fig. 6B, 6D, and 6F), with only a minor decrease in rest duration observed at 5 dpf (Fig. 6H). The low radiation group displayed increased activity but shorter activity bouts on 7 dpf (Fig. 6A and 6C), along with increased resting frequency on 5 dpf (Fig. 6E) and shorter resting bouts on days 5 and 7 (Fig. 6G). Notably, these distinctions ceased to exist by 8 dpf in both radiation groups.

III. DISCUSSION

This study provides new insights into the potential early neuroanatomical and behavioral effects of RF-EMR on zebrafish. Comparing our study with the studies of [14], [15], [16], and [17], we emphasize the importance of investigating a common frequency's impact within realistic exposure scenarios. By selecting a frequency of 900 MHz, commonly utilized in daily wireless technology, and accounting for the SAR beneath the water's surface, we closely replicated real-world human RF exposure scenarios.

Our observations of subtle behavioral and morphological changes in zebrafish reveal potential neurological effects of RF-EMR, thus advancing the understanding of non-thermal effects. Importantly, the changes observed were transient and did not persist past 8 dpf. Our study specifically focused on the developmental period of zebrafish embryos and our findings indicate that while non-thermal and reversible effects may exist, they are unlikely to significantly impact zebrafish embryos, even during this sensitive and vulnerable developmental phase. Additionally, our study suggests that during human development, babies are naturally shielded by the mother's body and fetus, potentially making them safer from RF-EMR. Similarly, adult humans, with increased protection from their skin and scalp, may experience minimal effects.

However, it is important to note that the exposure period in this study was limited to the first three days post-fertilization for zebrafish embryos. Further investigation is required to determine the potential effects of extended exposure periods, which may or may not yield more severe consequences that were not revealed in our study. Extrapolating our findings

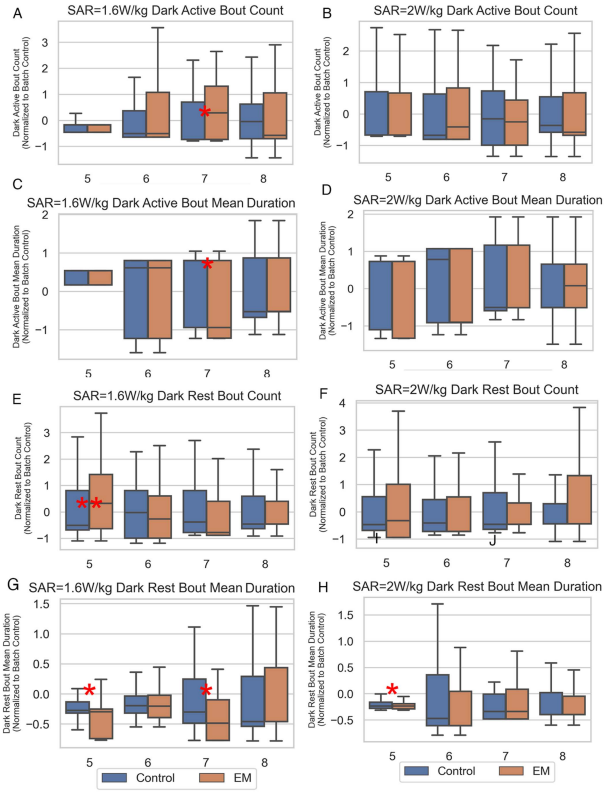

FIGURE 6. **Boxplots illustrating the active and rest bout counts and mean durations of active and rest bouts for zebrafish larvae after light OFF, at 5, 6, 7, and 8 dpf. Left: SAR = 1.6 W/kg; Right: SAR = 2 W/kg; Blue: control group; Orange: radiation group. Significance levels are denoted as follows: *** for $p < 0.001$, ** for $p < 0.01$, and * for $p < 0.05$.**

from zebrafish to human health necessitates careful consideration.

Additionally, we primarily compared the radiation groups with the environmental control group to conserve resources and space. However, this approach may not offer the same level of control as the sham-exposed group, which was identical to the experimental conditions except for the absence of EM-RF exposure. Future research should consider using both sham and environmental controls to more effectively isolate the effects of EM-RF exposure under different experimental settings.

In future studies, it is essential to expand our research by encompassing a broader range of frequencies and extended exposure duration. Moreover, delving into the potential mechanisms underlying the transient morphological and behavioral changes observed would provide valuable insights into the body's ability to reverse the effects of RF-EMR.

IV. CONCLUSION

In conclusion, our study marks a significant advancement in RF-EMR research, particularly within aquatic environments. We have developed an innovative platform capable of accurately simulating real-world exposure scenarios. Our research explored the effects of RF-EMR on zebrafish, specifically focusing on a frequency of 900 MHz, a frequency commonly found in everyday wireless technologies. We set the exposure levels to align with upper safety limits for public exposure from cellular telephones, providing a realistic representation of human exposure scenarios.

In contrast to previous research, this study comprehensively examined both neuroanatomical and behavioral changes in zebrafish, providing deeper insights into the impacts of RF-EMR. Our findings revealed that the exposure to RF-EMR led to minor increases in the sizes of the eye, whole-brain, and midbrain at certain developmental stages. Interestingly, we observed behavioral changes in the light-induced locomotor response assay, indicating potential alterations in alertness or stress levels. However, no visual impairments were detected, and these observed differences appeared to diminish by 8 dpf. This suggests that short-term exposure to RF-EMR does not cause permanent damage. Nevertheless, our study has laid a solid foundation for future investigations into the effects of long-term or continual exposure to RF-EMR. The implications of our research extend beyond academic inquiry, offering valuable insights for public health policy and the safe integration of wireless technologies in our environment.

In summary, our platform closely simulates real-world scenarios and can be easily adjusted to accommodate a wide array of common radio frequencies. The neuroanatomical and behavioral analysis serves as a robust tool for detecting potential changes in zebrafish larvae. By shedding light on the potential health risks associated with RF-EMR, our study highlights the importance of further exploration in this field, particularly considering the widespread use of wireless technologies in our modern environment.

V. METHODS

A. ELECTROMAGNETIC RADIATION SETUP

The establishment of uniform electrical fields (E-fields) within the water for zebrafish was facilitated through the utilization of the TBTC3 TEM cell from TEKBOX DIGITAL SOLUTIONS. This TEM cell is capable of confining the electromagnetic wave and creating a plane wave within a specific area. The RF generator (Aeroflex IFR 2052) was used for radiofrequency generation, and the power meter (Bird Electronic Corporation 4304 A) was employed to monitor the output to the TEM cell, maintaining a consistent radiation power level throughout the experiment. The input port of the TEM cell was linked to the power amplifier (Amplifier Research 25S1G4A) output port (Fig. 1A).

Four rectangular containers, each filled with embryo medium, were symmetrically positioned at the center of the TEM cell. The containers had a distance of 40 mm between each other and were oriented vertically in relation to the central and edged copper plates, allowing for more significant EM energy penetration into the embryo medium. The dimensions of the container were 124 mm × 17 mm × 10 mm (Figure S2), and the volume of the embryo medium within each container was 120 mm × 15 mm × 5 mm. The containers

were constructed from polylactic acid (PLA) material, featuring a permittivity of approximately 2.2, and were fabricated by 3D printing. Given the markedly lower permittivity of the container compared to the embryo medium ($\varepsilon_r = 81$), the container's impact on the RF-EMR within the water is negligible.

To assess the uniformity of the electromagnetic field (E-field), we utilized Ansys High Frequency Structure Simulator (Ansys-HFSS) to simulate the E-field of the TEM cell. The simulation setup is illustrated in Fig. 1A. In the simulation, we used specific materials for different components. The TEM Cell was made of aluminum, with a permittivity of 1, a conductivity of 3.8×10^7 siemens/m, and a thermal conductivity of 237 W/K/m. The container was composed of plexiglass, with a permittivity of 3.4, a conductivity of 0 S/m, and a thermal conductivity of 0.2 W/K/m. The zebrafish water was simulated as fresh water, with a permittivity of 81, a conductivity of 0.01 S/m, and a thermal conductivity of 0.6 W/K/m. To discretize the simulation model, we utilized a mesh consisting of 35,463 elements, as depicted in Figure S3.

In the simulation, the input power was adjusted to acquire the desired SAR value. The SAR value was estimated using the following equation:

$$SAR = \frac{\sigma E^2}{\rho} \tag{1}$$

where σ is the bulk conductivity of material, which is zebrafish tissue with an approximate 1 S/m. E symbolizes the magnitude of E-field in the water and ρ refers to the the mass density of embryonic zebrafish with an approximate 1 mg/mm^3 or 1000 kg/m^3 [22].

For SAR=2 W/kg, the optimized input power was identified as $Pin = 1.2\,W$. The magnitude of E-fields within the TEM cell, displayed in Fig. 1B, is approximately $44\,V/m$ and maintains a maintains a quasi-uniform trend within the water. An expanded view is shown on the right side of Fig. 1B.

To assess the thermal effects, thermal simulations were conducted using CST MICROWAVE STUDIO, as shown in Fig. 1C. The results demonstrated that the thermal effects were negligible, with the temperature beneath the water being comparable to the surrounding environment. Specifically, the temperature of the embryo medium was found to be approximately equal to the ambient temperature, which was set at $296.15\,K$. Similar observations were made for an SAR value of 1.6 W/kg, with an input power of $1\,W$.

It is worth noting that, in the experiment, the TEM cell was rotated 90 degrees counterclockwise. Moreover, this experimental setup can be scaled to accommodate different exposure frequencies and SAR levels.

B. RADIO FREQUENCY ELECTROMAGNETIC RADIATION EXPOSURE PROTOCOLS

Initially, we sterilized the electromagnetic radiation containers by immersing them in bleach for 2 hours. Subsequently, we rinsed the containers with water and placed them in embryo medium for 24 hours. We then prepared the zebrafish for spawning. For egg-laying, male and female fish (at a ratio of 1:1.5) were transferred to a breeding tank in the afternoon before fertilized eggs were required. A partition was used to keep them separated overnight, and this was removed the next morning. After about 1 h, newly fertilized embryos were collected, and the healthy embryoswere selected with a Leica stereoscopic microscope (Leica Zoom 2000, Germany) and incubated in E3 medium (5 mM NaCl, 0.17 mM KCl, 0.33 mM $CaCl_2$ and 0.33 mM $MgSO_4$) at 28 $\pm$ 0.5°C until required.

The healthy embryos were transferred to the containers that were placed inside the TEM cell for radiation exposure at two power levels, SAR=1.6 W/kg and 2 W/kg, while other containers were positioned outside the TEM cell (in the same room) to serve as the control group. We maintained consistent light and temperature conditions for both the radiation and control groups, recording the environmental temperature daily to ensure suitable conditions for zebrafish embryo development. The 54-hour RF-EMR exposure began at 4 hpf. On 1 dpf and 2 dpf, we changed the embryos medium in the container to maintain their freshness and removed any dead embryos. After the radiation exposure ended on 2 dpf, we transferred the embryos to a fish tank for 2 additional days of fertilization.

C. FISH HUSBANDRY

The zebrafish husbandry protocol was derived from [23]. The Tg(*elavl3: EGFP*)^{knu3} zebrafish lines used in this study were sourced from the China Zebrafish Resource Center (CZRC). These fish were maintained in 50 L glass tanks, with about 60 fish per tank, ensuring sufficient space and optimal water conditions. The tanks were kept at a stable temperature of 28 $\pm$ 1°C, with water pH maintained between 7 and 8. To support the natural circadian rhythms of the zebrafish, a consistent photoperiod of 14 hours of light and 10 hours of dark was adhered to daily. The water in the tanks was changed twice a week to maintain cleanliness and reduce stress, and the fish were fed twice daily with powdered food, supplemented with brine shrimp once a day. All procedures carried out with these live fish were performed in strict accordance with the guidelines set by the Animal Research Ethics Committee of City University of Hong Kong and the Department of Health, Hong Kong, ensuring ethical treatment and care throughout the study.

D. MORPHOLOGICAL STUDY

1) GROSS MORPHOLOGY

Prior to the commencement of the experiments, the zebrafish were randomly assigned to either control or treatment groups to ensure unbiased distribution. Fish exhibiting any malformations were identified and excluded from the study to avoid confounding factors. Zebrafish larvae aged 5—8 days dpf were embedded in a 2% low-melting-point agarose solution prepared in an embryo medium. To reduce movement artifacts, the solution included 0.08% MS222, an anaesthetic

agent. The larvae were then placed inside a glass capillary tube with a 1.5 mm internal diameter. Once the agarose solidified, the larvae were gently pushed out, positioned, and set on an agarose plate for imaging. A stereomicroscope was used to capture images of the larvae.

2) BRAIN MORPHOLOGY

To investigate the potential impact of RF-EMR exposure on brain development, we compared brain morphology between control and radiation groups during the period from 5 to 8 dpf. This analysis focused on identifying regional differences in morphology, as these variations may indicate varying sensitivity to RF-EMR exposure.

For visualization of the brain region in zebrafish larvae, Tg(*elavl3: EGFP*)^{knu3} was employed. Neurons are abundant in the brain. The Elavl3 transgenic zebrafish enables visualization of specific brain regions by expressing a fluorescent protein in mature neurons, effectively highlighting diverse neuronal populations in zebrafish larvae. To enhance the GFP signal in the Tg(*elavl3: EGFP*)^{knu3} transgenic line, immunofluorescence staining was performed. Zebrafish embryos aged 5-8 dpf were fixed in 4% paraformaldehyde (PFA) for 24 hours at -4°C, followed by five 3-minute washes with phosphate-buffered saline (PBS). The embryos were then dehydrated in a series of methanol solutions ranging from 50% to 100% and rehydrated in reverse order, spending 5 minutes in each concentration. Next, the embryos were washed three times for 15 minutes each with PBST (0.5% Tween-20 and 0.5% Triton X-100 in PBS) and blocked with MAXbind Staining Medium (Active Motif) for 1 h at room temperature. The samples were incubated with the 1:200 primary antibody (Mouse anti-GFP, A-21271; Invitrogen) overnight at 4°C, washed three times with PBST for 15 minutes each, and then incubated with the 1:1000 secondary antibody (Goat anti-Mouse IgG (H+L) Cross-Adsorbed Secondary Antibody, Alexa Fluor 488) overnight at 4°C. The embryos were washed again with PBST for 15 minutes three times and then with PBS for 5 minutes three times at room temperature before imaging.

Images were captured using a Zeiss Lightsheet Z.1 3D microscope, as previously described. After staining, the zebrafish larvae were embedded in 2% low-melting-point agarose within a small capillary glass tube with a 1.5 mm internal diameter. The tube was then placed in the microscope chamber, positioning the sample nearly vertically and aligning the back of the embryo's head parallel to the lens. The entire brain of the embryos was scanned using the Z-stack function, and images were exported after performing maximum projection. The experiments were meticulously replicated under identical conditions to ensure the statistical validity and reproducibility of the results. The different batches were combined into a larger group. The statistical comparison between the radiation group and control group was conducted on the combined data. A Mann-Whitney U test was employed for the statistical analysis. This approach allowed us to effectively compare the exposure group and control group, minimizing the influence of between-batch variation on our comparisons.

E. BEHAVIORAL STUDY

1) LIGHT-INDUCED LOCOMOTOR BEHAVIOR PARADIGM

The behavioral data were collected using a Zebrabox (Viewpoint Life Sciences). From 5 to 8 dpf, zebrafish larvae were placed in a 96-well plate and then transferred to a dark Zebrabox for 30 minutes of dark adaptation. This initial phase aimed to familiarize the zebrafish with the experimental environment. Then the subsequent OFF phase enabled the larvae to establish a baseline level of activity. After the baseline OFF phase, a bright light stimulus was applied following an ON-OFF-ON-OFF sequence, with each stimulus phase lasting for 30 minutes, as illustrated in Figure S1. The movements of the larvae were detected by an infrared camera, capturing videos at a rate of 30 frames per second.

In this study, we aimed to measure movement by defining and detecting burst duration using a specific extraction scheme. First, detection sensitivity was established to compare two consecutive frames and identify active pixels, which are characterized by a change in gray level greater than the detection sensitivity. We adjusted the detection sensitivity to 10, aiming to exclusively register zebrafish movement while ignoring unrelated environmental noise. The active pixels correspond to larval movement between successive frames. Subsequently, a burst threshold was determined to define actual movement (i.e., burst) when the number of active pixels between two frames surpassed a predefined value. The burst duration was then defined as the total duration of actual movement per second, or the fraction of a second in which a larva genuinely moves (bin size as 1 s). We tested burst thresholds (BT=4), consistent with previous studies [21], [24], [25], [26]. To avoid any effects from background changes, the background refresh was set to occur every 60 seconds. The larval movement data were collected from 5 dpf to 8 dpf.

To strengthen the reliability of our behavioral data and minimize the impact of extraneous factors, we employed a sham control approach in conjunction with our main experiments. The sham control group underwent the same handling and procedural steps as the radiation groups, with the key distinction being the absence of electromagnetic EM-RF exposure. Specifically, embryos in the sham control group were housed in identical TEM cell and maintained under the same environmental conditions as the radiation groups, except the TEM cell was not activated.

To economize on costs and space, we evaluated the behavioral patterns of the sham control group and the environmental control group, both composed of embryos from the same batch and located in the same room as the radiation groups. The key distinction was that the sham control group was placed inside the TEM cell, while the environmental control group was not. According to our supplementary data (Figure S4-S5), there were no significant differences in behavioral patterns between these groups. Thus, for simplicity and to

maintain consistent batch and temperature conditions, our analysis primarily focused on comparing the radiation groups with the environmental control group.

2) BEHAVIOR RELATED METRICS AND DEFINITION

To analyze the behavioral patterns, we considered two aspects: the pre- and post- stimulus burst activities and behavioral patterns extracting from bursting activities.

For comparing the pre- and post- stimulus burst activities, we selected the 60-second-long segments, which included 30 s before and 30 s after the stimulus changes. We removed the baseline activities, batch activities, and well-dependent activities using a similar approach as in [27]. By applying a linear regression with batch and well factors, we predicted the bursting activities. Subsequently, we subtracted the predicted activities explained by the batch and well from the actual bursting activities. Furthermore, we removed the individual larva's baseline activities by subtracting the mean bursting activities from the 30 seconds before the stimuli. Finally, we compared the activities between the exposure group and the control group using the Hotelling's T-squared test.

For the analysis of behavioral patterns, we collected features from the burst activity data pertaining to the initial switch from OFF to ON, as well as from ON to OFF. The specific features that we gathered for this analysis are delineated in Table S1. The startle response, which occurs within 3 seconds following light activation, is defined as a burst activity greater than three standard deviations above the pre-light ON activity. We calculated the ratio of larvae exhibiting startle responses and the time bin when these responses occurred. Startle response-related parameters signify larvae reaction to sudden changes in illumination, reflecting their visual capability and adaptability to environmental changes.

We defined the bout count and mean bout duration for both active and rest periods as follows: the last 10 minutes of both light-on and light-off periods as the stable period. The mean activity level and the standard deviation during this stable period establish the baseline activity for both light-on and light-off periods. During both light and dark phases, any bursts of activity exceeding two standard deviations above the baseline activity were categorized as active bouts. Conversely, periods falling below two standard deviations from the baseline activity were termed as rest bouts. When calculating the bout counts, any bouts occurring consecutively were counted as one bout. To derive the mean bout duration, we divided the total duration of bouts of the same kind by the bout count.

In order to mitigate the impact of between-batch variation, we applied normalization to the data. This was achieved by first subtracting the mean of the respective variable in the control group (which came from the same batch as the exposure group) and then dividing the result by the control group's standard deviation. After normalization, the different batches were combined into a larger group. The statistical comparison between the exposure group and control group was conducted on the combined data. This normalization approach allowed us to effectively compare the exposure group and control group, minimizing the influence of between-batch variation on our comparisons. To assess the differences in the incidence of startle responses between the exposure and control groups from days 5 to 8 dpf, we conducted a chi-square test for each day's data. For analyzing other behavioural features, we initially evaluated the distribution of data for normality within each group using the Shapiro-Wilk test. Due to the data exhibiting non-normal distributions, we opted for a non-parametric method, employing the Mann-Whitney U test for comparisons between the two groups.

SUPPLEMENTARY MATERIAL

Included in the supplementary materials are Table S1-S5 and Figure S1-S5. Table S1 presents the definitions of bursting features, while Tables S2, S3, and S4 provide the sample sizes per group and developmental stage for gross morphological analysis, brain morphological analysis, and behavioral analysis, respectively. Table S5 offers a statistical comparison between the sham control and control groups, specifically examining power levels and days with pre-stimulus and post-stimulus p-values. Figure S1 depicts the light-induced locomotor behavior paradigm, describing the experimental setup and tracking time. Figure S2 illustrates the dimensions of the container used for holding zebrafish embryos during electromagnetic radiation exposure. Figure S3 shows the mesh used in the simulation model for the TEM cell. Figures S4 and S5 focus on the behavioural analysis for the control and sham control groups under different conditions. Readers are encouraged to review the supplementary materials to gain more details.

AUTHOR CONTRIBUTIONS

Xiaoli Wu conducted data analysis, performed a literature review, visualized data, and wrote and edited the draft. Yu Suen Chan collected data, visualized data, and wrote the draft. Bingjie Xiang designed and constructed the TEM cell, conducted data simulation experiments, and visualized data. Wenhui Zhang conducted data analysis and collected data. Kwai-Man Luk provided critical guidance throughout experiments and offered critical suggestions during manuscript writing. Shuk Han Cheng provided guidance throughout experiments and offered suggestions during manuscript writing. Yuk Fai Leung provided essential recommendations for experiments, contributed to draft writing and editing, and conceptualization. Rosa H. M. Chan initiated the project, conceptualized the study, developed the methodology, edited the draft, and managed the project.

CONFLICT OF INTEREST

The authors of this manuscript declare no conflicts of interest.

REFERENCES

[1] S. N. Narayanan, R. Jetti, K. K. Kesari, R. S. Kumar, S. B. Nayak, and P. G. Bhat, "Radiofrequency electromagnetic radiation-induced behavioral changes and their possible basis," *Environ. Sci. Pollut. Res.*, vol. 26, pp. 30693–30710, 2019.

[2] A. ICNIRP, A. Ahlbom, A. Green, L. Kheifets, L. Savitz, and A. Swerdlow, "Epidemiology of health effects of radiofrequency exposure," *Environ. Health Perspectives*, vol. 112, no. 17, pp. 1741–1754, 2004. [Online]. Available: https://ehp.niehs.nih.gov/doi/abs/10.1289/ehp.7306

[3] A. B. Miller et al., "Risks to health and well-being from radio-frequency radiation emitted by cell phones and other wireless devices," *Front. Public Health*, vol. 7, 2019, Art. no. 223.

[4] S. Ohtani et al., "Exposure time-dependent thermal effects of radiofrequency electromagnetic field exposure on the whole body of rats," *J. Toxicolog. Sci.*, vol. 41, no. 5, pp. 655–666, 2016.

[5] *Centers Dis. Control Prevention*, "Radiofrequency (rf) radiation," 2023, Accessed: Jun. 3, 2023. [Online]. Available: https://www.cdc.gov/nceh/radiation/radiofrequency-radiation.html

[6] P. Wust et al., "Non-thermal effects of radiofrequency electromagnetic fields," *Sci. Rep.*, vol. 10, no. 1, 2020, Art. no. 13488.

[7] D. Belpomme, L. Hardell, I. Belyaev, E. Burgio, and D. O. Carpenter, "Thermal and non-thermal health effects of low intensity non-ionizing radiation: An international perspective," *Environ. Pollut.*, vol. 242, pp. 643–658, 2018.

[8] N. D. Volkow et al., "Effects of cell phone radiofrequency signal exposure on brain glucose metabolism," *Jama*, vol. 305, no. 8, pp. 808–813, 2011.

[9] J. J. McGill and A. Agarwal, *The Impact of Cell Phone, Laptop Computer, and Microwave Oven Usage on Male Fertility*. New York, NY, USA: Springer, 2014, pp. 161–177.

[10] L. Roshangar, B. Hamdi, A. Khaki, J. S. Rad, and S. Soleimani-Rad, "Effect of low-frequency electromagnetic field exposure on oocyte differentiation and follicular development," *Adv. Biomed. Res.*, vol. 3, 2014, Art. no. 76.

[11] J. A. Adams, T. S. Galloway, D. Mondal, S. C. Esteves, and F. Mathews, "Effect of mobile telephones on sperm quality: A systematic review and meta-analysis," *Environ. Int.*, vol. 70, pp. 106–112, 2014.

[12] A. Wdowiak et al., "Effect of electromagnetic waves on human reproduction," *Ann. Agricultural Environ. Med.*, vol. 24, no. 1, 2017, pp. 13–18.

[13] Statista, "Statistics & facts on wearable technology," 2023. [Online]. Available: https://www.statista.com/topics/1556/wearable-technology/

[14] C. C. Piccinetti et al., "Measurement of the 100 mhz emf radiation in vivo effects on zebrafish d. rerio embryonic development: A multidisciplinary study," *Ecotoxicol. Environ. Saf.*, vol. 154, pp. 268–279, 2018.

[15] S. Dasgupta et al., "Impacts of high dose 3.5 ghz cellphone radiofrequency on zebrafish embryonic development," *PLoS One*, vol. 15, no. 7, 2020, Art. no. e0235869.

[16] V. Nassisi et al., "Zebrafish larval melanophores respond to electromagnetic fields exposure," *Appl. Sci.*, vol. 13, no. 8, 2023, Art. no. 4721.

[17] Y. Guo, Y. Fu, and W. Sun, "50 hz magnetic field exposure inhibited spontaneous movement of zebrafish larvae through ros-mediated Syn2a expression," *Int. J. Mol. Sci.*, vol. 24, no. 8, 2023, Art. no. 7576.

[18] Federal Communications Commission, "Specific absorption rate (SAR) for cellular telephones," 2023, Accessed: Dec. 29, 2023. [Online]. Available: https://www.fcc.gov/general/specific-absorption-rate-sar-cellular-telephones

[19] International Commission on Non-Ionizing Radiation Protection, "Guidelines for limiting exposure to electromagnetic fields (100 khz to 300 ghz)," 2020, Accessed: Dec. 29, 2023. [Online]. Available: https://www.icnirp.org/cms/upload/publications/ICNIRPrfgdl2020.pdf

[20] World Health Organization, "Electromagnetic fields and public health: Mobile phones" 2021. [Online]. Available: https://www.who.int/news-room/fact-sheets/detail/electromagnetic-fields-and-public-health-mobile-phones

[21] Y. Gao et al., "A high-throughput zebrafish screening method for visual mutants by light-induced locomotor response," *IEEE/ACM Trans. Comput. Biol. Bioinf.*, vol. 11, no. 4, pp. 693–701, Jul.–Aug. 2014.

[22] D. Poljak and M. Cvetković, "Simplified models of the human body," in *Human Interaction with Electromagnetic* F. D. Poljak and M. Cvetkovi ć., Eds. New York, NY, USA: Academic Press, 2019, pp. 91–122.

[23] M. Westerfield, *The Zebrafish Book: A Guide for the Laboratory Use of Zebrafish (Danio Rerio)*. Eugene, OR: Univ. Oregon Press, 2000.

[24] J. Rihel et al., "Zebrafish behavioral profiling links drugs to biological targets and rest/wake regulation," *Science*, vol. 327, no. 5963, pp. 348–351, 2010.

[25] F. Emran, J. Rihel, A. R. Adolph, K. Y. Wong, S. Kraves, and J. E. Dowling, "Off ganglion cells cannot drive the optokinetic reflex in zebrafish," *Proc. Nat. Acad. Sci.*, vol. 104, no. 48, pp. 19126–19131, 2007.

[26] Y. Gao et al., "Computational classification of different wild-type zebrafish strains based on their variation in light-induced locomotor response," *Comput. Biol. Med.*, vol. 69, pp. 1–9, 2016.

[27] R. Xie et al., "Normalization of large-scale behavioural data collected from zebrafish," *PLos One*, vol. 14, no. 2, 2019, Art. no. e0212234.